

Gyrokinetic Simulations of Slab Ion Temperature Gradient Turbulence with Kinetic Electrons^{*)}

Akihiro ISHIZAWA, Tomo-Hiko WATANABE and Noriyoshi NAKAJIMA

National Institute for Fusion Science, 322-6 Oroshi-cho, Toki 509-5292, Japan

(Received 22 December 2010 / Accepted 9 May 2011)

Ion temperature gradient (ITG) driven turbulence is investigated by means of gyrokinetic simulations which include both kinetic ions and electrons in slab geometry with uniform equilibrium magnetic field. The study confirms that numerical results satisfy the entropy balance equation including both ions and electrons. The entropy variable is transferred from ions to electrons through the perturbation of electrostatic potential, and the transferred fluctuation is diffused by the electron collision dissipation. In the ITG turbulence with kinetic electrons ion heat diffusion is larger than that with adiabatic electrons. The former is close to the latter when the ion mass is comparable to or larger than the hydrogen one. The difference between the transport coefficients does not originate from the suppression of turbulence by zonal flow, but stems from the difference between their spectra. The lowest wavenumber mode dominates the coefficient in the adiabatic electron case, while the transport is caused not only by the lowest mode but by higher wavenumbers in the kinetic electron cases.

© 2011 The Japan Society of Plasma Science and Nuclear Fusion Research

Keywords: turbulence, gyrokinetic simulation, kinetic ion, kinetic electron

DOI: 10.1585/pfr.6.2403087

1. Introduction

The ion temperature gradient (ITG) instability has been studied as the mechanism of anomalous ion heat transport [1]. The nonlinear mode coupling causes micro-turbulence called the ITG turbulence, and also produces coherent poloidal flows called zonal flows that regulate the turbulence by its shear motion [2]. The ITG turbulence regulated by the zonal flow has been extensively studied by means of gyrokinetic simulations. In gyrokinetic simulations of ITG turbulence the adiabatic response of electrons is usually assumed. This assumption stems from the fact that the electron mass is much smaller than the ion mass. The electrons move much faster than ions along the magnetic field lines, and the distribution is close to the Maxwell-Boltzmann equilibrium, so that electrons respond adiabatically to the potential. On the other hand, the adiabatic response of ions is usually assumed in simulations of electron temperature gradient (ETG) driven turbulence. This adiabatic response is caused by the fact that typical spatial scale of ETG is much smaller than the ion Larmor radius. Recently, it is claimed that introduction of kinetic ion dynamics is critical to the electron heat transport in the toroidal ETG turbulence in large magnetic shear case [3]. The results motivate us to study turbulence by means of gyrokinetic simulations including both kinetic ions and electrons. Such simulations are applied to the studies of trapped-electron mode turbulence [4] and turbulence in finite beta plasmas [5-7].

author's e-mail: ishizawa@nifs.ac.jp

^{*)} This article is based on the presentation at the 20th International Toki Conference (ITC20).

In this paper, as the first step, we focus on the non-adiabatic response of electrons in the slab ITG turbulence. We investigate the ITG turbulence by means of gyrokinetic simulations which include both kinetic ions and electrons in a slab geometry. The thermal transport caused by ITG turbulence with kinetic electrons is compared to that with adiabatic electrons.

2. Simulation Model

We consider a radially localized region of a slab plasma in an uniform magnetic field and assume that plasma beta is zero. The magnetic field is $\vec{B} = B_0(\vec{e}_z + \theta\vec{e}_y)$ with $\theta \ll 1$. Temperature and density gradients are uniform and direct to x -axis, and temperature gradient which causes the ITG instability is represented by the parameter $\eta_s = L_n/L_{T_s}$ in terms of density scale length $L_n = -(\mathrm{d} \ln n / \mathrm{d} x)^{-1}$ and temperature scale lengths $L_{T_s} = -(\mathrm{d} \ln T_s / \mathrm{d} x)^{-1}$, where the subscript s denotes species. The distribution function is assumed to be the Maxwellian distribution in v_\perp space, $F_s(\vec{x}, v_\parallel)F_{sM\perp}(v_\perp)$. By dividing the distribution function into the Maxwellian part and a perturbation part, $F_s(\vec{x}, v_\parallel) = F_{sM}(v_\parallel) + \delta f_s(\vec{x}, v_\parallel)$, and integrating the gyrokinetic equations over v_\perp , we obtain the gyrokinetic equations of perturbed distribution functions of ions and electrons

$$\frac{\partial \delta f_{sk}}{\partial t} + \frac{ik_y \Theta v_{\parallel s}}{\sqrt{\tau_s M_s}} \delta f_{sk} + \sum_{k', k''} \delta_{k'+k'', k} \vec{e}_z \cdot \vec{k}' \times \vec{k}'' \delta \Phi_{sk'} \delta f_{sk''}$$

$$= C_s(\delta f_{sk}) - ik_y F_{sM} \delta \Phi_{sk} (q_s \sqrt{\frac{\tau_s}{M_s}} \Theta v_{\parallel s} - v_{*s}), \quad (1)$$

and gyrokinetic Poisson equation,

$$\lambda_{Di}^2 k_{\perp}^2 \delta \phi_k = \sum_s \left(q_s \int \delta f_{sk} e^{-b_{sk}/2} dv_{\parallel s} - \tau_s [1 - \Gamma_0(b_{sk})] \delta \phi_k \right), \quad (2)$$

in the Fourier space. In Eq. (1) we define the function

$$v_{*s} = -1 - (v_{\parallel s}^2 - 1 - b_{sk}) \frac{\eta_s}{2},$$

and use the collision operator

$$C_s(\delta f_{sk}) = \nu_s \frac{\partial}{\partial v_{\parallel s}} \left(\frac{\partial}{\partial v_{\parallel s}} + v_{\parallel s} \right) \delta f_{sk},$$

$\delta \Phi_{sk} = \delta \phi_k e^{-b_{sk}/2}$, $\Gamma_0(b_{sk}) = e^{-b_{sk}} I_0(b_{sk})$, $b_{sk} = M_s k_{\perp}^2 / \tau_s$, $k_{\perp}^2 = k_x^2 + k_y^2$, $F_{sM}(v_{\parallel}) = e^{-v_{\parallel}^2/2} / \sqrt{2}$, $q_i = 1$, $q_e = -1$, where ν_s and I_0 are the collision frequency and the zeroth order modified Bessel function, respectively. The normalizations used in the dimensionless Eqs. (1) and (2) are $(t\nu_{Ti}/L_n, k\rho_{Ti}, v_{\parallel}/v_{Ts}, F_{sM}\nu_{Ts}/n_0, \delta f_s L_n \nu_{Ts}/(\rho_i n_0), \delta \phi_e L_n/(\rho_i T_i), \theta L_n/\rho_i, m_s/m_i, T_i/T_s, n/n_0, B/B_0, q_s/e, \lambda_{Di}/\rho_i) \rightarrow (t, k, v_{\parallel s}, F_{sM}, \delta f_s, \delta \phi, \Theta, M_s, \tau_s, n, B, q_s, \lambda_{Di})$, where $v_{Ts} = \sqrt{T_s/m_s}$, $\rho_i = v_{Ti}/\Omega_i$, $\lambda_{Di} = \sqrt{T_i/(4\pi e^2 n_0)}$.

The simulation domain is in (x, y) plane in the configuration space and the box size is L_n . The periodic boundary conditions are assumed in the space and the Fourier decomposition is used. The number of the mode is 256×256 . Time integrations are made by the fourth-order Runge-Kutta-Gill method and the $v_{\parallel s}$ derivative is approximated by a finite-difference method. In the $v_{\parallel s}$ direction, 128 grid points are uniformly distributed. The initial amplitudes of distribution functions are 10^{-4} , their phases are random in the Fourier space, and their profiles are a Maxwellian distribution in the velocity space.

We remark that the adiabatic electron response means that the two terms that are proportional to $ik_y \Theta v_{\parallel s}$ dominate in the electron equation of Eq. (1), i.e. $ik_y \Theta v_{\parallel e} \delta f_{ek} = ik_y \Theta v_{\parallel e} F_{eM} \delta \Phi_{ek} / \tau_e$. When the adiabatic response of electrons is valid Eqs. (1) and (2) are reduced to the set of gyrokinetic equations in Ref. [8].

3. Simulation Results

We consider a plasma which is unstable against the ITG instability. We set $\eta_i = 10$, $\eta_e = 0$, $\Theta = 1.2$, $\nu_s = 5 \times 10^{-4}$, $\tau_e = 1$, $\lambda_{Di} = 0$, and $L_n = 20\pi\rho_i$.

The slab ITG instability produces strong zonal flow, and thus the amplitude of turbulence is small and zonal flow dominates as shown in Fig. 1 which shows electrostatic potential profile at $t = 820$ for the mass ratio $m_i/m_e = 1836$. Because of the strong zonal flow the ion thermal transport coefficient normalized by the gyro-Bohm coefficient is very small.

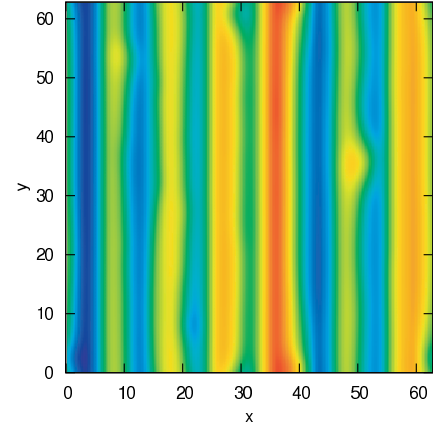


Fig. 1 Color map of electrostatic potential of slab ITG turbulence at $t = 840$ in a quasi-steady state for $m_i/m_e = 1836$.

3.1 Entropy balance

The entropy balance equation for species s is obtained from Eq. (1) and is written as

$$\frac{d\delta S_s}{dt} - \eta_s Q_s - \Gamma_s - D_s = R_s, \quad (3)$$

where

$$\begin{aligned} \delta S_s &= \sum_k \int dv_{\parallel s} \frac{|\delta f_{sk}|^2}{2F_{sM}(v_{\parallel})\tau_s}, \\ Q_s &= Re \left[- \sum_k \frac{ik_y \delta \phi_k e^{-b_{sk}/2}}{2\tau_s} \int dv_{\parallel s} \delta f_{sk}^* \frac{1}{2} (v_{\parallel s}^2 - 1 - b_{sk}) \right], \\ \Gamma_s &= Re \left[- \sum_k \frac{ik_y \delta \phi_k e^{-b_{sk}/2}}{2\tau_s} \int dv_{\parallel s} \delta f_{sk}^* \right], \\ D_s &= \sum_k \int dv_{\parallel s} \frac{\delta f_{sk}^* C_s}{F_{sM}}. \end{aligned}$$

The entropy variable exchange between ions and electrons is represented by

$$R_s = \frac{1}{\sqrt{\tau_s M_s}} Re \left(\sum_k q_s \delta u_{\parallel sk}^* \delta E_{\parallel sk} \right),$$

where $\delta u_{\parallel sk} = \int dv_{\parallel s} v_{\parallel s} \delta f_{sk}^*$ and $\delta E_{\parallel sk} = -ik_y \Theta \delta \phi_k e^{-b_{sk}/2}$. We remark that only the non-adiabatic part of δf_{sk} contributes to R_s . The entropy balance equation is obtained from Eqs. (1) and (2) and is written as

$$\begin{aligned} &\sum_s \left(\frac{d\delta S_s}{dt} - \eta_s Q_s - \Gamma_s - D_s \right) + \frac{dW}{dt} \\ &= \sum_s R_s + dW/dt = 0, \end{aligned} \quad (4)$$

where

$$W = \sum_{s,k} \left(\lambda_{Di}^2 k_{\perp}^2 + q_s^2 \tau_s [1 - \Gamma_0(b_{sk})] \right) \frac{|\delta \phi_k|^2}{2}.$$

Figure 2 shows time evolution of each term in the entropy balance equation Eq. (4) for the mass ratio $m_i/m_e = 1836$.

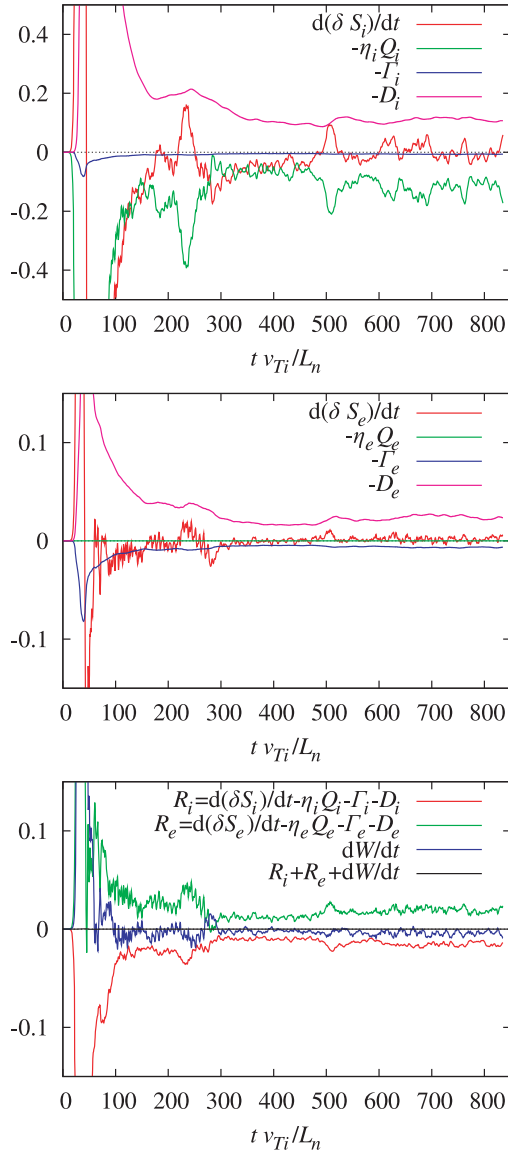


Fig. 2 Time evolution of each term in the entropy balance equation Eq. (4) for the mass ratio $m_i/m_e = 1836$.

In order to reduce fast oscillation we plot the value averaged from $t - 5$ to $t + 5$ in the figure. Since the turbulence is driven by ITG, the terms from the equation of ion distribution function are much larger than those from the electron equation. The ion heat flux Q_i nearly balances with ion collision diffusion D_i in the quasi-steady state $t > 500$. We remark that the particle flux Γ_i is finite because of kinetic electrons, but it is small. The electron particle flux Γ_e is also small and similar to Γ_i , and does not balance with the electron collision diffusion D_e . Thus, the electron entropy variable exchange $R_e = d\delta S_e/dt - \eta_e Q_e - \Gamma_e - D_e$ is positive. This R_e balances with the ion entropy variable exchange $R_i = d\delta S_i/dt - \eta_i Q_i - \Gamma_i - D_i$ which is negative. The sum of them $\sum_s R_s$ and the potential energy term dW/dt completely balances, and hence the entropy balance equation Eq. (4) is satisfied. The balance between R_i and R_e implies that the perturbation of electrostatic potential

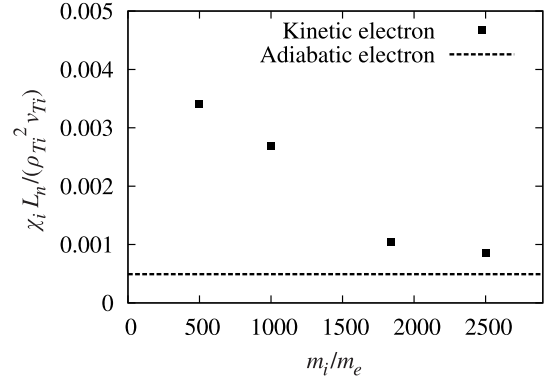


Fig. 3 Time-averaged thermal transport coefficient as a function of the mass ratio m_i/m_e . In this and following figures the time-average is made in the quasi-steady state which is achieved, for instance, after $t = 300$ for the mass ratio $m_i/m_e = 1836$ case.

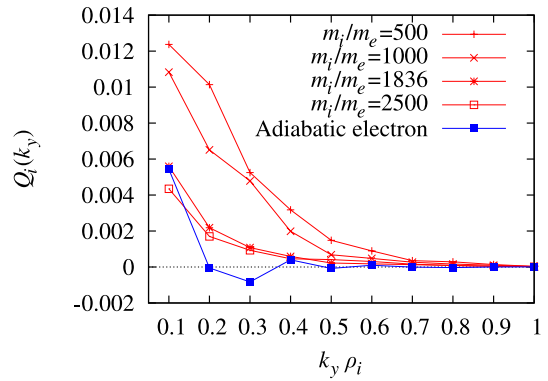


Fig. 4 Time-averaged spectra of heat transport.

due to ITG fluctuates the electron distribution, and thus the entropy variable is transferred from ions to electrons. The transferred fluctuation is almost dissipated by the electron collision diffusion, $R_e - D_e \approx 0$, because fine-scale structures of electron distribution function in the velocity space are generated by the convection in the phase space.

3.2 Ion heat transport and zonal flow

Figure 3 shows the mass ratio dependence of the time-averaged ion heat transport coefficient in the radial direction $\chi_i = Q_i/\eta_i$ which is normalized by the gyro-Bohm coefficient. The coefficients are averaged over time in the quasi-steady state which is achieved, for instance, after $t = 300$ for the $m_i/m_e = 1836$ case. The coefficients χ_i with the kinetic electrons are larger than that with the adiabatic electrons, but is close to the latter when the mass ratio is large. The spectra of heat flux averaged over time in the quasi-steady state is shown in Fig. 4. The lowest wavenumber mode $k_y \rho_i = 0.1$ dominates the spectrum for the adiabatic electron case. On the other hand, the spectra are finite not only at the lowest wavenumber mode but also higher wavenumbers $k_y \rho_i > 0.1$ in the kinetic electron case. The difference is reduced when the mass ratio is larger than that of hydrogen. The clear difference of spectra does not

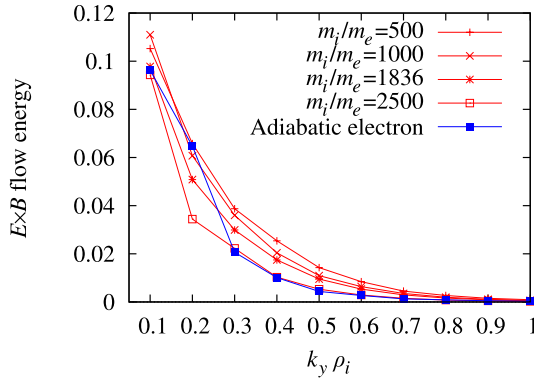


Fig. 5 Time-averaged spectra of $E \times B$ flow energy, $\sum_{k_x} |\vec{k} \delta \phi(k_x, k_y)|^2 / 2$

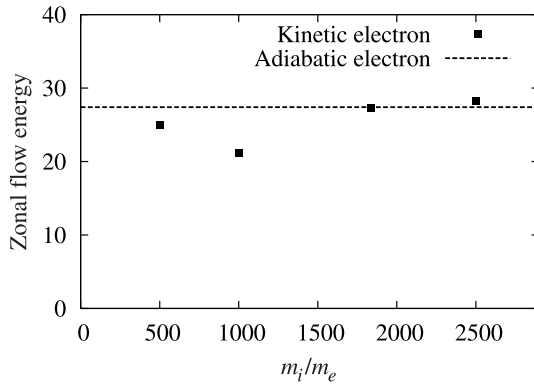


Fig. 6 Time-averaged zonal flow energy, $\sum_{k_x} \langle |i\vec{k} \delta \phi(k_x, k_y)|^2 \rangle / 2$, as a function of the mass ratio.

appear in the energy spectra. Figure 5 shows the energy spectra of $E \times B$ flow energy $\sum_{k_x} |\vec{k} \delta \phi(k_x, k_y)|^2 / 2$ averaged over time in the quasi-steady state. The spectra are similar to each other for the adiabatic and kinetic electron cases. Thus, we infer that the difference between the spectra of heat transport is not caused by the difference in the amplitude of the fluctuations but in the phase lag between the potential and temperature fluctuations.

Figure 6 shows the mass ratio dependence of zonal flow energy $\sum_{k_x} \langle |i\vec{k} \delta \phi(k_x, k_y)|^2 \rangle / 2$, where $\langle \rangle$ stands for the average over y . We do not see any tendency in the mass ratio dependence of zonal flow energy.

4. Summary and Discussion

We have constructed a gyrokinetic simulation code including both kinetic ions and electrons in slab geometry and studied the effects of kinetic electrons on slab ITG driven turbulence.

We obtained a quasi-steady state of ITG turbulence and firstly presented the numerical solution that satisfies the entropy balance equation for ion and electron species. The ion heat flux almost balances with the ion collision dissipation. The ion particle flux is finite because of kinetic electrons, but it is quite small. The electron particle flux is also quite small and does not balance with the electron

collision dissipation making the sum of the electron parts positive. This positive sum balances with entropy variable exchange of ions, and thus the entropy variable is transferred from ions to electrons through the electrostatic potential perturbation. The transferred fluctuation is almost diffused by the electron collision dissipation.

The time-averaged ion thermal transport coefficient with kinetic electrons is larger than that with adiabatic electrons and decreases as the mass ratio m_i/m_e increases. It is close to that obtained by assuming the adiabatic response of electrons, when the ratio is equal to or larger than that of hydrogen. This suggests that the thermal transport slightly decreases when the ratio increases from that of hydrogen to deuterium in the slab ITG turbulence. In spite of the fact that the energy spectra of ITG with kinetic electrons are not so different from that with adiabatic electrons, the spectra of heat flux in case with kinetic electrons is considerably different from that with adiabatic electrons. A plausible explanation is that the phase difference between the electrostatic potential and temperature fluctuations in ITG turbulence with kinetic electrons deviate from that in case with adiabatic electrons.

The present study has shown no clear dependence of the zonal flow amplitude on the ion-electron mass ratio, and it remains to be clarified how the zonal flow generation influences small values of the ion heat transport in the slab ITG turbulence. Here, it should be reminded that there is no dissipation mechanism of zonal flows in the slab plasmas, while very strong zonal flows are produced in the slab ITG turbulence with no neoclassical polarization effect. Thus, generally speaking, the choice of the initial condition may affect the details of the zonal flow generation process at least in the early saturation phase of the instability growth, and hence, the resultant zonal flow amplitude. Recent slab ETG turbulence simulation [9] showed that the tilt angle of the magnetic field, Θ , influences the zonal flow amplitude. The dependence of the zonal flow production on Θ and the initial perturbations is left for future studies.

The authors would like to thank Professor W. Horton for careful reading of this paper.

- [1] W. Horton, Rev. Mod. Phys. **71**, 735 (1999).
- [2] P.H. Diamond, S.-I. Itoh, K. Itoh and T.S. Hahm, Plasma Phys. Control. Fusion **47**, R35 (2005).
- [3] R.E. Waltz, J. Candy and M. Fahey, Phys. Plasmas **14**, 056116 (2007).
- [4] T. Dannert and F. Jenko, Phys. Plasmas **12**, 072309 (2005).
- [5] J. Candy, Phys. Plasmas **12**, 072307 (2005).
- [6] M.J. Pueschel, M. Kammerer and F. Jenko, Phys. Plasmas **15**, 102310 (2008).
- [7] M.J. Pueschel and F. Jenko, Phys. Plasmas **17**, 062307 (2010).
- [8] T.-H. Watanabe and H. Sugama, Phys. Plasmas **11**, 1476 (2004).
- [9] M. Nakata, T.-H. Watanabe, H. Sugama and W. Horton, Phys. Plasmas **17**, 042306 (2010).